2

QUANTUM DOT-SENSITIZED SOLAR CELLS (QDSSCs)[*]

2.1 Introduction

Renewable energy has been a global issue in recent years. Due to many issues such as limited fossil fuel reserve and global warming, the need for renewable energy cannot be denied. An alternative that has emerged as a potential and marketable source of energy is solar. In an hour, a total of 4.3×10^{20} J energy from the sun that reaches the earth is sufficient to fulfill the global energy consumption in a year (4.1×10^{20} J) [1]. Energy fom the sun can be easily trapped using low-cost and high-efficiency solar cells. A wide range of solar cell technologies which includes dye-sensitized nanocrystalline solar cells [2], bulk heterojunction solar cells [3,4], depleted heterojunction solar cells [5,6], and hybrid organic-inorganic solar cells [7-9] are being researched and developed.

---

[*] Portions of this chapter were published in: Jun, H.K., Careem, M.A. & Arof, A.K. (2013). Quantum dot-sensitized solar cells – perspective and recent developments: A review of Cd chalcogenide quantum dots as sensitizers. *Renewable and Sustainable Energy Reviews,* 22, 148-167.

Chronologically, solar cell technologies have evolved into three generations [10]. The first generation photovoltaic cells are based on a single crystalline semiconductor wafer. The second generation photovoltaic solar cells utilize inorganic thin film structure in the cell assembly. They are cheaper to produce, but the efficiency, which is less than 14% in amorphous thin film solar cells is lower than the efficiency exhibited by the single junction crystalline photovoltaic cell of the first generation that can reach as high as 27% (see Figure 1.1 in Chapter 1). Theoretically, single junction cells should be able to exhibit a maximum efficiency of ~33% [11], a limit set by Shockley-Queisser thermodynamics. Thus, a new solar cell technology is required in order to achieve efficiencies greater than 33% with lower production cost. The onset of this breakthrough is the third generation photovoltaic cells [12]. The relation between the photovoltaic production cost per square metre with the solar cell module efficiency and the cost per unit power are shown in Figure 2.1 [13]. It is predicted that with the emergence and advancement of the third generation photovoltaic cells, higher efficiency devices are possible with lower production cost. Some examples of solar cells which fall under this category are dye-sensitized solar cells (DSSCs), quantum dot-sensitized solar cells (QDSSCs), colloidal quantum dot solar cells (CQD), organic solar cells, etc.

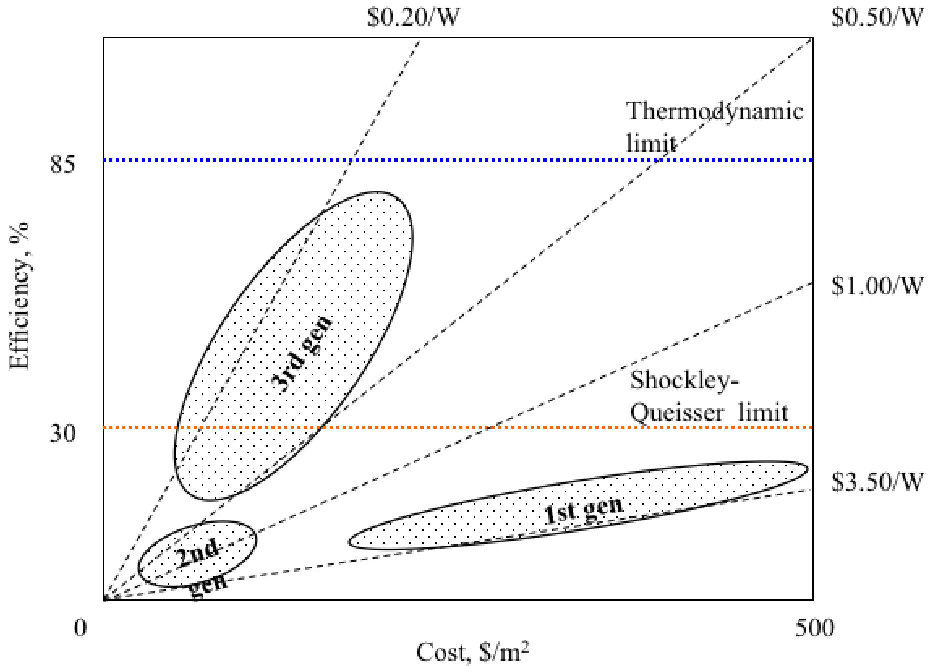

Figure 2.1 Efficiency-cost trade-off for the three generations of solar cell technology; wafers, thin-films and advanced thin-films (year 2003 dollars). Adapted from reference [13].

The first low-cost and high-efficiency solar cells introduced were the DSSCs with inorganic ruthenium based dyes in the early 90s [14]. From then onwards, numerous research have been focused on the development and characterization of different dyes for DSSC application. These include natural [15,16] and synthetic organic dyes [17]. Based on the DSSC's structure, quantum dot (QD) was introduced to replace the dye due to its excellent opto-electronic properties [2,18,19]. QDs are nano-sized semiconductor particles whose physical and chemical properties are size-dependent. Among the notable characteristics of QDs include tunability of band gap energy, narrow emission spectrum, good photostability, broad excitation spectra, high extinction coefficient and multiple exciton generation [20-23]. With these advantages, researchers were able to fabricate solar cell devices achieving efficiency up to 7% in QD related solar cells [24,25]. Other upcoming trend is "green" QDSSC where less hazardous precursors are used during the preparation of QDs [26].

Over the last few years, cadmium chalcogenide (CdX, X = S, Se or Te) QDs have attracted more attention in QDSSC research. The widespread of research activities in CdX QDs are due to their distinct properties such as ease of fabrication, tunability of band gap energy through size control and possible multiple exciton generation as mentioned above. It is noted that CdX absorbs photon efficiently because it has a bulk material band gap above 1.3 eV (band gap for CdS, CdSe and CdTe are 2.25 eV, 1.73 eV and 1.49 eV respectively) [27]. By altering the QD size, the band gap can be tuned further to match a desired band gap range. It is therefore critical to understand the physics and chemistry of these CdX QDs for a better research focus.

This literature review though inexhaustive will concentrate on the concepts of the QDSSC with emphasis on cadmium chalcogenide (CdX, X= S, Se or Te) as QD sensitizers. The fundamental electrical characteristics of solar cells will be first reviewed. This will be followed by basic working principles of the QDSSC. Subsequent sections are dedicated to the synthesis methods and sensitization with CdX QDs.

2.2 Basic principles of QDSSCs

2.2.1 Structure of DSSC and QDSSC

A typical DSSC consists of a dye-sensitized photoanode (working electrode) and a counter electrode (CE) separated by a salt electrolyte [28]. Photoanode consists of a mesoporous wide-bandgap semiconductor layer that is attached to the conducting glass. Typically, TiO_2 is chosen for the mesoporous semiconductor although other oxides such as ZnO and Nb_2O_5 are possible [19,29,30]. A monolayer of charge transfer dye is then attached on the surface of the mesoporous wide-bandgap semiconductor. This photoanode section is in contact with a redox electrolyte or hole conductor. The structure is completed by coupling with a counter electrode (cathode) as shown in Figure 2.2.

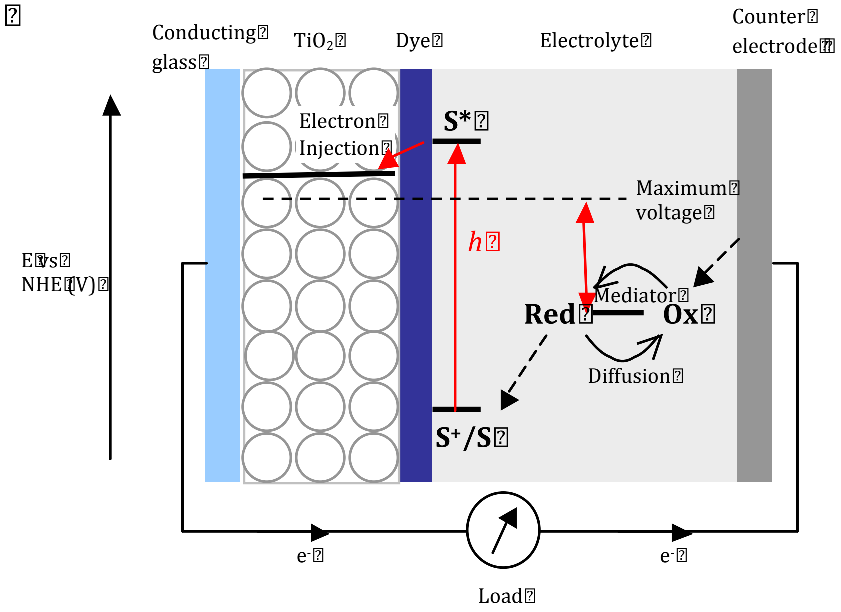

Figure 2.2 Structure and operating principle of a typical DSSC. Adapted from reference [28].

The evolution of DSSC to QDSSC does not take a big leap. The only physical difference between the DSSC and QDSSC is the sensitizing materials. In the QDSSC, the dye is replaced by inorganic QD nanoparticles [31]. The mesoporous TiO_2 is coated using colloidal QD or *in situ* fabricated QDs [18,32-34]. The working mechanism of the solar cell is further explained in section 2.2.3.

2.2.2 Performance parameters

The function of a conventional photovoltaic solar cell is based on the formation of an electrical barrier between n- and p-type semiconductors. The potential difference across this barrier creates an electrical diode structure. Thus, the current-voltage characteristic of the solar cell follows the diode equations. Figure 2.3 is an illustration of current-voltage characteristics of a solar cell in the dark and under illumination conditions.

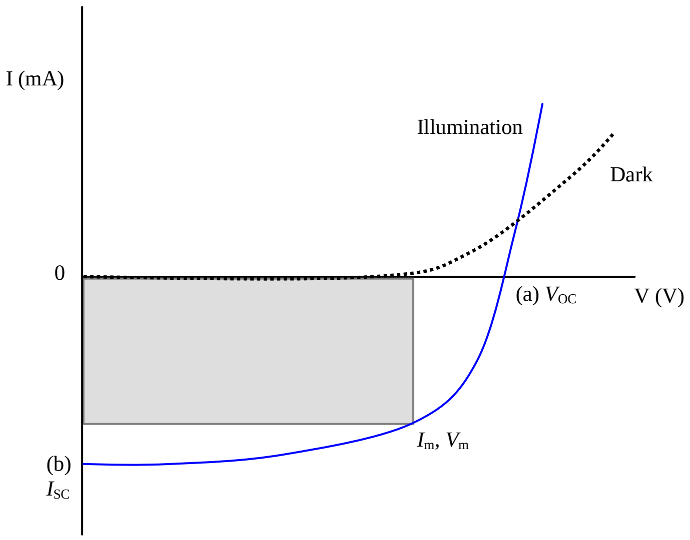

Figure 2.3 Current-voltage curves of a photovoltaic solar cell under dark and illuminated conditions. The intersection value with the abscissa and ordinate are the open-circuit voltage (V_{oc}) and the short-circuit current (I_{sc}) respectively. Maximum power output, P_{max} is determined by the maximized product of I_m and V_m. By dividing the P_{max} with the product of I_{sc} and V_{oc}, it results the fill factor (FF).

Under the dark condition, there is no current flowing. However, when a sufficiently high voltage is applied i.e. higher than open circuit voltage, the contacts start to inject carriers to produce current at forward bias. Upon illumination, additional photocurrent will be generated to flow across the junction. The maximum generated photocurrent contributes to the short-circuit current (I_{sc}). The open-circuit voltage (V_{oc}) is the voltage when there is no current flowing. Power output then can be determined from the product of current and voltage in the fourth quadrant of the current-voltage characteristics. At the maximum power point (I_m and V_m), the product is the largest, where the maximum rectangle area in the figure meets the curve [7]. This defines the fill factor (FF).

$$\mathrm{FF} = (I_m \times V_m) / (I_{sc} \times V_{oc}) \qquad (2.1)$$

The maximum theoretical FF value is 1.0 or 100%. However, in reality the value is limited to 0.83 based on the diode equation [1]. The photovoltaic power conversion efficiency, η, is defined by the electrical power density divided by the incident solar power density (P). P is standardized at 1000 Wm^{-2} for photovoltaic cell tested at spectral intensity matching the sun's intensity on earth's surface at an angle of 48.2° (equivalent to AM 1.5 spectrum) [7].

$$\eta = I_m \times V_m / \mathrm{P} \tag{2.2a}$$

$$\eta = I_{sc} \times V_{oc} \times \mathrm{FF} / \mathrm{P} \tag{2.2b}$$

QDSSCs also function like junction solar cells under dark and illuminated conditions and therefore, their performance parameters can also be obtained using the above equations.

In a three-electrode measurement, conversion efficiency is measured as incident photon to current efficiency (IPCE). IPCE is a measure of ratio of charge carriers collected at the electrodes to the number of incident photons, also known as external quantum efficiency. IPCE at different wavelengths is determined from the short circuit photocurrents (I_{sc}) observed at different excitation wavelengths using the expression [7]:

$$\mathrm{IPCE}\ \% = (1240 \times I_{sc}) / (\lambda \times I_{inc}) \times 100 \tag{2.3}$$

where I_{inc} is the incident light power (i.e. the energy of the light incident on the electrode) and λ is wavelength. For an ideal solar cell, the I_{sc} value can be determined from the IPCE data with the standard AM 1.5 spectrum. However, in QDSSC, the case is not ideal. Thus the calculated I_{sc} might be an approximation for the measured I_{sc} under 1 sun (1000 Wm^{-2}) [21].

2.2.3 Working mechanism

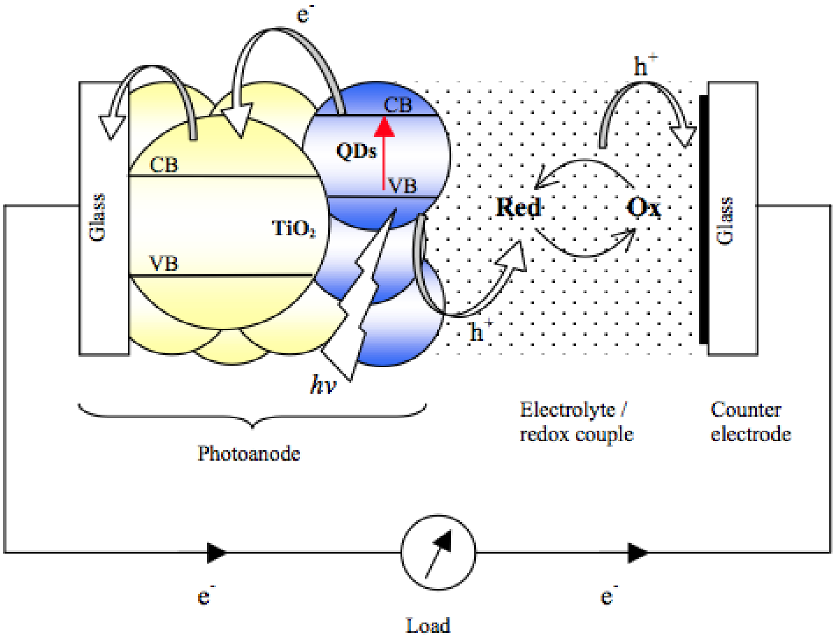

Figure 2.4 Structure and operating principle of a typical QDSSC. Adapted from reference [20].

A general structure of a QDSSC and its operation is depicted in Figure 2.4. The working mechanism of the QDSSC is very similar to that of the DSSC. When the QDs (CdX, X = S, Se or Te) are subjected to band gap excitation, upon illumination, electron-hole pairs are formed in the QDs. The electrons will enter into the conduction band (CB) of the QD and the hole remains in the valence band (VB). The excited QD injects the electron from its CB into the CB of the wide-bandgap semiconductor (e.g. TiO_2) and in doing so it itself is oxidized with the hole remaining in the valence band. The injected electron from the QD percolates through the porous TiO_2 network and ultimately reaches the conducting glass. From there it travels through the external load and completes the circuit by entering back through the counter electrode. The generated voltage is perceived as an evidence of the solar energy conversion to electric energy. This voltage corresponds to the difference between the quasi-Fermi level of the electron in the photoanode and the redox potential of the polysulfide electrolyte [30], which usually consists of a (S^{2-}/S_x^{2-}) redox couple. The oxidized QD is then restored (hole is filled with electron) when it is reduced by S^{2-} from the electrolyte and in turn it is oxidized back into S_x^{2-} that diffuses to the counter electrode. Chemically, the following reactions take place where oxidation occurs at the photoanode-electrolyte interface [35]:

$$S^{2-} + 2h^+ \rightarrow S \tag{2.4}$$

$$S + S_{x-1}^{2-} \rightarrow S_x^{2-} \text{ (x = 2 to 5)} \tag{2.5}$$

At the counter electrode, reduction occurs where the S_x^{2-} is reverted back to S^{2-}:

$$S_x^{2-} + 2e^- \rightarrow S_{x-1}^{2-} + S^{2-} \tag{2.6}$$

The whole key processes of the photocurrent generation can be illustrated as in Figure 2.5. It should be concluded that QDs have a photovoltaic response upon illumination which results in photocurrent and voltage generation. They have the tendency of charging up to a state that changes the relative energetics within the cell which ultimately influence the generation and recombination processes [36].

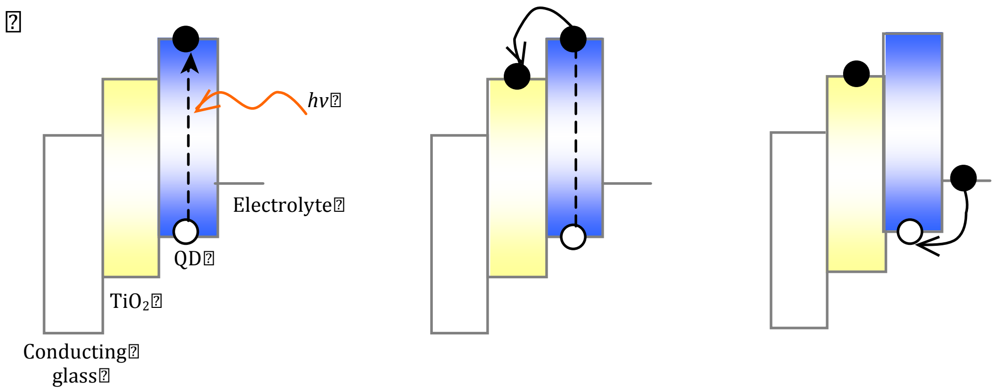

(a) Light absorption (b) Electron transfer (c) QD neutralization

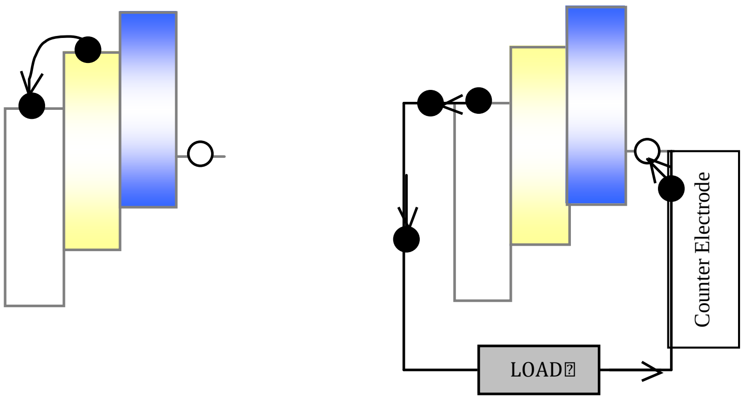

(d) Electron transport (e) Electrolyte regeneration

Figure 2.5 Schematic of an energy diagram of a QDSSC stack under flat band conditions. Key processes leading to the generation of photocurrent are shown in (a) – (e). Illustration is based on the concept in reference [35].

2.3 Transport processes and properties of QDSSC

2.3.1 Charge separation and transport

In the DSSC, charge separation occurs at the interface between wide-bandgap semiconductor/dye and electrolyte. For QDSSC, charge separation reactions are at the surface between the wide-bandgap semiconductor/QD and redox electrolyte. Upon illumination, the excited QDs will generate electron-hole pairs [37-39]:

$$CdX + h\nu \rightarrow CdX(e + h) \qquad (2.7)$$

where e and h denote electron and hole generated respectively. At the interface between TiO_2 and the excited QDs, charge transfer takes place:

$$CdX(e+h) + TiO_2 \rightarrow CdX(h) + TiO_2(e) \qquad (2.8)$$

$$CdX(h) + Red \rightarrow CdX + Ox \qquad (2.9)$$

where Red and Ox are the reduced and oxidized conditions of the electrolyte. Thus, for CdX-TiO_2 system with polysulfide redox couple, reaction (2.9) can be expressed as:

$$CdX(h) + S^{2-} \rightarrow CdX + S \rightarrow CdX + S_x^{2-} \qquad (2.9a)$$

It was reported that the electron transfer is size-dependent especially in QD-TiO_2 system and that the charge injection dynamics are determined by the QDs [39]. Different pH electrolyte solution could also modulate the charge injection process when in contact with the photoanode as observed in fluorescence spectra reported by Chakrapani *et al.* [40]. They observed that the CB of TiO_2 shifted to more negative potentials at higher pH value (more alkaline). This resulted in a decrease of the energy difference between CB band edges of QD and TiO_2. Consequently, electron injection rate would be decreased. One interesting point to take note is that there’s no significant difference in the electron injection and recombination of injected electrons on the sizes of the QDs [41].

2.3.2 Advantages of quantum dots (QDs) as sensitizers

Some of the advantages of QDs are tunable energy gaps, ability of multiple exciton generation, good photostability, low cost and high absorption coefficient, which is known to reduce the dark current and increase the overall efficiency of the solar cells [42]. Of all these, tunable energy gaps and multiple exciton generation features are the most desirable characteristics of the QDs [20-23].

2.3.2.1 Tunable energy gaps

The feasibility of QDs as sensitizers in QDSSC have been studied by various groups [22,23,31,43]. All the QD properties mentioned in the preceding sections are not only limited to Cd chalcogenides but applicable to other QD materials as well. The main motivation of using QDs as sensitizers in solar cell is due to their tunable energy band gaps, which can control their absorption range [19]. There are several reports in the literature showing that CdS and CdSe with tunable band gaps property are capable of converting visible light to electric energy [39,44]. Vogel *et al.* demonstrated that efficient charge separation can be optimized by tuning the size of the QDs utilizing the quantization effect [19]. Kongkanand *et al.* separately reported that by varying the size of CdSe QDs assembled on TiO_2 films, improvement in photoelectrochemical response and photoconversion efficiency can be obtained (Figure 2.6) [39]. With the decrease of CdSe particle size, photocurrent increases due to the shift of the CB to more negative potentials which in turn increases the driving force for charge injection. As a result, higher IPCE is obtained at the excitonic band. On the other hand, QD particles will have better absorption in the visible region with the increase of particle size. The disadvantage of this is lower effectiveness of electron injection into TiO_2 as compared with smaller-sized CdSe QDs.

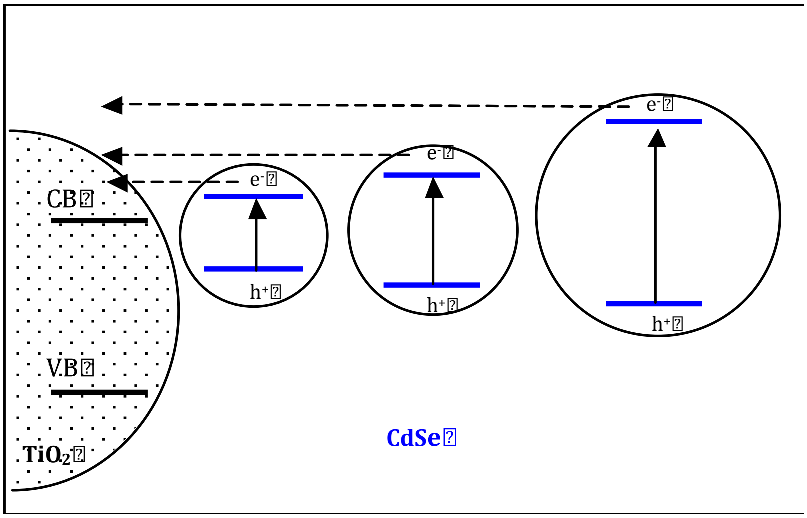

Figure 2.6 Schematic diagram illustrating the energy levels of different-sized CdSe QDs and TiO_2. (The injection of electrons from CdSe QDs into TiO_2 is influenced by the energy difference between the two conduction bands. Note that band positions are for reference only and not to scale). Adapted from reference [39].

This size dependent effect is made possible due to the quantum confinement effect exhibited by the QD itself [43,45]. Quantum confinement effect can be manifested when QDs in colloidal solution show different colour corresponding to the change of particle size, which influences a different absorption band of light. When the QD particles are sufficiently small, the effective band gap energy of the QD is wider. Subsequently, the optical absorptions and emissions in relation with excitations across the band gap shift towards higher energies [21]. Quantum size effects have been demonstrated by Gorer *et al.* with the observed blue shift of the optical spectra of CdSe films as the crystal size decreases [46]. This phenomenon is also highlighted in CdS QDs as reported by Thambidurai *et al.*, where the same blue shift was observed in the optical spectra of smaller CdS QDs [47]. Therefore, it can be concluded that a combination of different QD sizes in a cell will have better efficiency due to wider absorption of light by the QDs which have different range of band gaps.

2.3.2.2 Multiple exciton generation

Multiple exciton generation (MEG) in QDs from a single photon have been studied previously by some groups [31,48-54]. MEG is the generation of more than one electron-hole pair upon the absorption of a photon. This phenomenon was first demonstrated in PbS and PbSe QDs systems in year 2004-2005 [48-50]. However, subsequent studies revealed that multiple exciton generation has not been detected in CdSe and CdTe QDs systems [55] although some latest investigations showed the possibility [53,56,57]. The process could be mediated by different mechanisms in CdSe nanoparticles. Essentially, multiple excitons are generated when hot carriers produce more than one electron-hole pair through impact ionization.

Upon absorption of solar radiation, photon with energies greater than the band gap creates electrons and holes. At this point, the excess kinetic energy is equal to the difference between the photon energy and the band gap, which creates an effective temperature condition for the carriers. The temperature of the carriers is higher than the lattice temperature. Thus, the term hot carriers (or hot electrons and hot holes) is used. It is predicted that an efficient multiple exciton generation can enhance the conversion efficiencies of QDSSC up to 44% [58]. More details of MEG can be found in the review by Nozik [31].

2.4 Preparation of QD sensitizers

There are various methods for preparing QDs and attaching them to the wide-bandgap semiconductor material [59]. Generally, these methods can be categorized into two major methods: *in situ* fabrication and attachment of pre-synthesized colloidal QD. *In situ* fabrication method is the most used approach for QDs preparation. It is facile and low cost. Chemical bath deposition (CBD) and successive ionic layer adsorption and reaction (SILAR) are two well known *in situ* techniques. Not only the techniques are simple, but they also can be used in large scale production. However, these techniques do not allow precise control of the particle size distribution of the QDs.

The other approach is to use pre-synthesized QDs (also known as *ex situ* fabrication). QDs are usually prepared *ex situ* and adsorbed on the wide-bandgap semiconductor surface by using molecular linkers that have various functional groups. QDs can also be deposited directly without using linker molecules. This technique enables the precise control over the size and hence the spectral absorption properties of the QDs.

2.4.1 Chemical bath deposition (CBD)

In this method, nucleation and growth of QDs take place in one bath. Cationic and anionic solutions are prepared separately and placed in a container to form a bath solution. QDs are grown on the surface of the wide-bandgap semiconductor on an electrode surface by dipping the electrode into the bath solution for a defined period. Thus, the QDs deposition is controlled by varying the dipping time. This method has been used to attach CdS and CdSe QDs onto wide-bandgap semiconductors [33] although the reaction is slow. Recently, a new type of CBD approach has been introduced which is referred to as sequential CBD (S-CBD) [60]. This method is however, very similar to SILAR method described below. In a latest development, microwave assisted CBD is used and this method is capable of producing QDs that can improve the short circuit current density as well as power conversion efficiency in QDSSCs [61,62]. Here the deposition of QDs is done with TiO_2 electrode immersed into a sealed container containing a precursor aqueous solution. The container is then put into a microwave system for a suitable microwave treatment. The addition of the microwave step can spur faster nucleation and growth of QDs. Zhu *et al.* [61,62] claim that this procedure enable fast deposition of CdS layer which assists in suppressing carrier recombination at the surface defects of QDs as well as facilitate easy attachment of QDs.

2.4.2 Successive ionic layer adsorption and reaction (SILAR)

SILAR method is an extension of CBD technique [63]. In this approach, cationic and anionic precursors are separately placed in two beakers or containers. TiO_2 coated electrode is dipped into the cationic precursor solution followed by rinsing and drying. Then it is dipped into the anionic precursor solution and completed with a final rinsing and drying. The two-step dipping is regarded as one deposition or SILAR cycle. The size of the deposited QDs can be controlled by the number of dip cycles. Within a cycle, each dipping period can be tailored to achieve the desired particle size growth. The overall SILAR process can be illustrated as in Figure 2.7. This method is designed such that the particle size will increase by one monolayer during a dip or immersion cycle. SILAR is a better approach when compared with CBD because of its shorter processing time and close stoichiometry formation as reported by Senthamilselvi *et al.* [64]. This method has been successfully utilized to grow CdS, CdSe and CdTe QDs on the TiO_2 film [65,66]. In a recent work by Barcelo *et al.*, SILAR has been shown to be advantageous when applied to ZnO mesoporous electrode due to its simplicity, homogenous QD distribution, high QD coverage degree and high IPCE values obtained in QDSSCs [67].

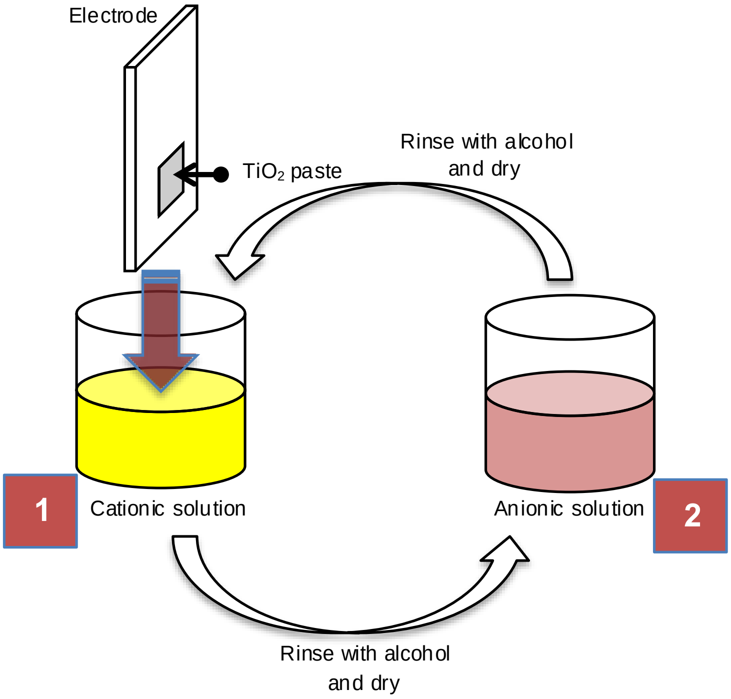

Figure 2.7 Illustration of SILAR process where QD is grown on the substrate by successive dipping and drying.

2.4.3 Surface attachment through molecular linker for *ex situ* fabrication of QDs

For QD deposition via surface attachment, QDs are first pre-synthesized using capping agents. Capping agents are responsible in controlling the nanostructure shape, size and optical properties. Some examples of capping agent are mercaptopropionic acid (MPA), trioctylphosphine (TOP) and trioctylphosphine oxide (TOPO). Synthesis is performed in a vessel where the metal precursor (e.g. CdO) is heated before the inclusion of the next organometallic precursor (e.g. TOP-Se solution). Removing the heat will stop the growth reaction. In other words, QD size is controlled via temperature and also the capping agent concentration. The QD growth needs to be monitored using UV/Vis spectroscopy. Thus, a series of experiments should be performed to determine the size of the QDs formed at specific temperature and concentration of the capping agent. After the QDs are synthesized, the wide-bandgap semiconductor coated electrode is immersed in a solution containing bifunctional molecular linkers (in this case is the capping agent such as MPA). The immersion causes the functional group of the linker to attach onto the semiconductor surface while the other end of the functional group is available for QD attachment. Functional linking molecules assist in dispersing and stabilizing the QDs more effectively [68]. Subsequent immersion of the semiconductor electrode in a solution containing the QDs is required to allow the adsorption of QDs onto the semiconductor film surface. The immersion may last from few hours to a few days, which is a very time consuming process as compared with CBD or SILAR method. During the QD solution immersion, ligand exchange takes place. Figure 2.8 shows a schematic diagram of the process of molecular linking with QD and TiO_2 surface. Synthesis of CdX (X = S, Se, Te) using linker via wet chemical route has been first demonstrated by Murray *et al.* [69].

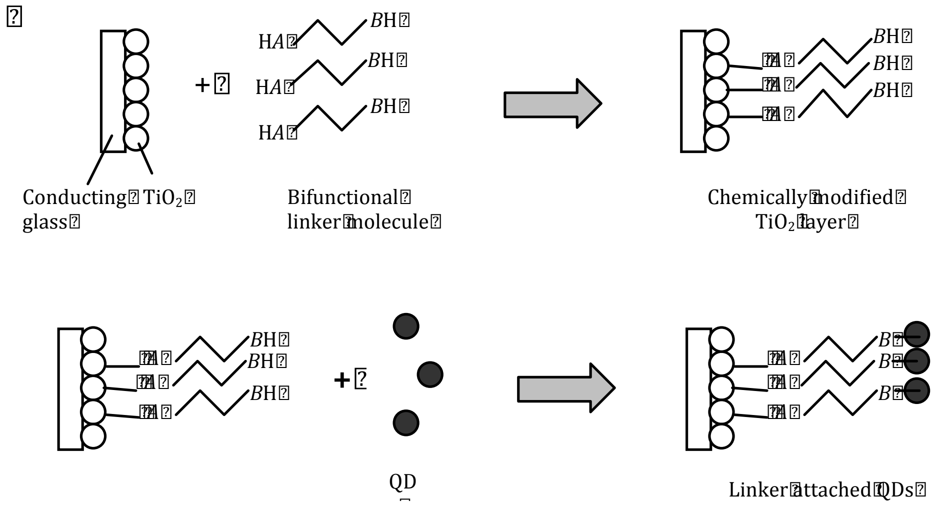

Figure 2.8 Linking QDs to TiO_2 surface with a bifunctional molecular linker. Adapted from reference [37].

2.4.4 Other methods

Besides CBD, SILAR and linker assisted assembly, QDs can also be prepared and attached via direct adsorption (DA) or physisorption. In DA, QDs are attached on the wide-bandgap semiconductor film without the assistance of a molecular linker. DA may lead to a high degree of QD aggregation in addition to a low surface coverage [70,71]. Interestingly, QDs prepared by DA method give higher IPCE values in QDSSCs compared to those obtained with QDs prepared with molecular linker assisted adsorption as reported by Guijarro *et al.* [71]. In their work, an IPCE of 36% at the QD excitonic peak was observed.

A less explored technique, physisorption, has been reported in the review by Rühle *et al.* [21]. In this technique, bare semiconductor electrodes (e.g. TiO_2, ZnO) are dipped into solution of QDs up to 100 hours. Literature regarding this technique is somewhat limited. Nevertheless, photovoltaic cell performance with QDs attached via physisorption indicates a better result than the performance of cell with QDs prepared using molecular linker assisted adsorption.

In Wijayantha *et al.*'s work [72], CdS QDSSCs were assembled via a pressing route where a polymer film was placed on the top of the CdS deposited TiO_2 layer, and the electrode was subsequently pressed between the two plates. The photoanode prepared via the pressing route has a tendency of experiencing partial loss or damage of the CdS layer. This method may also create regions that are inaccessible to the redox electrolyte. According to the authors, pressing route gives an alternative low cost method for the preparation of QD-sensitized photoelectrodes.

Electrophoretic deposition, another new deposition technique which was used recently by Salant *et al.* [73] in 2010 has been able to generate high power conversion efficiency in CdSe QDSSCs. The reported efficiency of 1.7% at 1 sun was higher than those of the cells with QDs prepared with a linker technique. Interestingly, the absorbed photon to electron conversion efficiencies is not size dependent, which means that efficient electron injection can take place for larger QD sizes. Poulose *et al.* [74] have adopted a combination method of functional linker with electrophoretic deposition to fabricate CdSe QDs. This method has the advantage of obtaining better QD deposition onto TiO_2 layers with reduced deposition time. This opens an alternative route for efficient QD deposition.

QDs can also be prepared via spray pyrolysis deposition (SPD) [75-77]. In the case of a CdS QDSSC reported by Lee *et al* [75], CdS QD was deposited onto the TiO_2 layer via SPD using solution mixture of cadmium chloride and thiourea. The deposited CdS layer had a porous structure. The photoelectrode was then subjected to washing to remove the excess cadmium chloride. The performance of the QDSSC with QDs prepared by this technique is comparable with those of the cells prepared by other existing techniques. The good performance was mainly attributed to the large surface area of the formed CdS in contact with the electrolyte. Due to required high temperature (above 400°C) in the process coupled with low QDSSC performance, this method is not widely used by researchers. Other new alternative methods include electro-spray technique and spin-coating-based SILAR [78,79]. In electro-spray technique, QDs suspension is prepared and loaded in a syringe. A syringe pump feed the suspension through the needle at a constant flow rate. High voltage is applied to the needle so that a cone-jet is formed at the needle outlet. QDs suspension is then sprayed onto the TiO_2 film which is set perpendicular to the needle. This method is very similar to electrospinning method. In spin-coating-based SILAR, both anionic and cationic precursors are dropped onto the TiO_2 film surface. The sample is then spin-coated without rinsing and drying process. This process is repeated few times until a desired QD layer is formed. Spin-coating-based method proves to be simple and fast as compared with normal SILAR method. However, much optimization work is needed to obtain a comparable cell performance with the cell containing QDs prepared from normal SILAR method.

2.5 Characterization of QDSSC

QDSSC device characterization can be grouped into 2 categories: steady state characterization and dynamic study (Figure 2.9). Steady state characterization is the most common method employed for basic solar cell characterization. Techniques used in this study include *I-V* curve measurement, UV-vis spectroscopy analysis and external quantum efficiency (IPCE) measurement.

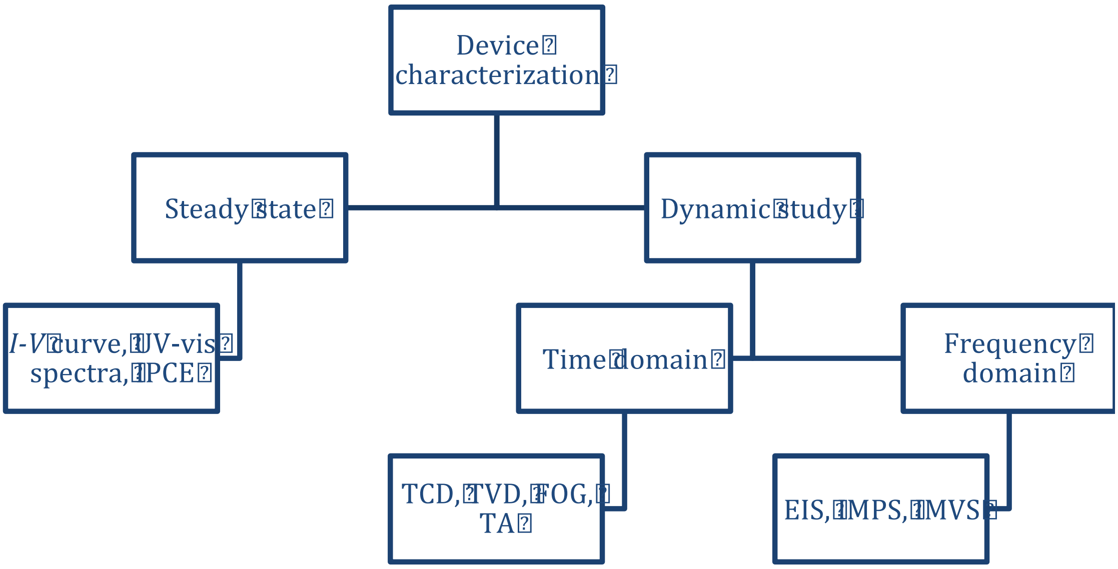

Figure 2.9 Device characterization technique for QDSSC.

To further understand the physics behind the solar cell performance, dynamic study of the device is required. The study can be carried out either in time domain technique or frequency domain technique. Under time domain study, the most widely used techniques are charge extraction method, transient photocurrent decays (TCD), transient photovoltage decays (TVD) and ultrafast spectroscopy analysis (FOG, TA). On the other hand, frequency domain study is also popular due to its simple and fast data interpretation. The techniques include electrochemical impedance spectroscopy (EIS), intensity-modulated photocurrent spectroscopy (IMPS) and intensity-modulated photovoltage spectroscopy (IMVS). Some of the techniques used in this thesis work are further explained in Chapter 3.

2.6 Summary

QDSSCs have become a promising alternative for DSSCs due to the excellent properties of QD sensitizers. Among the wide variety of semiconductor materials available for QDs, Cd chalcogenide has been the preferred choice for many researchers, especially CdS and CdSe. Research activities have been focused in improving the overall efficiency of the QDSSC in recent years. In order to achieve improvements and breakthroughs in QDSSCs performance, focus should be channeled to the investigation of materials, surface treatments of photoanode and combined absorbers [80]. Given the limited range of materials that have been investigated so far, there are more avenues to explore and understand the use of new materials in improving the performance of QDSSCs. It is forecast that the efficiency of QDSSCs could achieve higher value at lower cost should the trend of third generation solar cell materialise. Although the power conversion efficiencies achieved are relatively high as reported in some articles, the variation in the reported values is mainly due to various methods and parameters used in each research. This implies the possibility of more novel discoveries and innovative research in the near future. Nevertheless, the highest efficiency obtained has been increasing from year to year.

2.7 References

[1] Lewis, N.S., & Crabtree, G. (2005). *Basic research needs for solar energy utilization. In: 2005 Report on the Basic Energy sciences Workshop on Solar Energy Utilization.* Retrieved from U.S. Department of Energy website: http://www.er.doe.gov/bes/reports/files/SEU_rpt.pd

[2] Grätzel, M. (2003). Dye-sensitized solar cells. *Journal of Photochemistry and Photobiology C: Photochemistry Reviews, 4,* 145-153.

[3] Blom, P.W.M., Mihailetchi, V.D., Koster, L.J.A., & Markov, D.E. (2007). Device physics of polymer: Fullerence bulk heterojunction solar cells. *Advanced Materials, 19,* 1551-1566.

[4] Peumans, P., Uchida, S., & Forrest, S.R. (2003). Efficient bulk heterjunction photovoltaic cells using small-molecular-weight organic thin films. *Nature, 425,* 158-162.

[5] Kramer, I.J., Zhitomirsky, D., Bass, J.D., Rice, P.M., Topuria, T., Krupp, L., *et al.* (2012). Ordered nanopillar structured electrodes for depleted bulk heterojunction colloidal quantum dot solar cells. *Advanced Materials, 24,* 2315-2319.

[6] Pattantyus-Abraham, A.G., Kramer, I.J., Barkhouse, A.R., Wang, X., Konstantatos, G., Debnath, R., *et al.* (2010). Depleted-heterojunction colloidal quantum dot solar cells. *ACS Nano, 4,* 3374-3380.

[7] Gunes, S., & Sariciftci, N.S. (2008). Hybrid solar cells. *Inorganica Chimica Acta, 361,* 581-588.

[8] McGehee, M.D. (2009). Nanostructured organic-inorganic hybrid solar cells. *MRS Bulletin, 34,* 95-100.

[9] Chandrasekaran, J., Nithyaprakash, D., Ajjan, K.B., Maruthamuthu, S., Manoharan, D., & Kumar, S. (2011). Hybrid solar cell based on blending of organic and inorganic materials – an overview. *Renewable and Sustainable Energy Reviews, 15,* 1228-1238.

[10] Werner, J.H. (2004). Second and third generation photovoltaics – dreams and reality. *Advances in Solid State Physics, 44,* 51-67.

[11] Shockley, W., & Queisser, H.J. (1961). Detailed balance limit of efficiency of p-n junction solar cells. *Journal of Applied Physics, 32,* 510-519.

[12] Green, M.A. (2000). Prospect for photovoltaic efficiency enhancement using low-dimensional structures. *Nanotechnology, 11,* 401-405.

[13] Green, M.A. (2006). *Third Generation Photovoltaics: Advanced Solar Energy Conversion.* Berlin: Springer-Verlag.

[14] O’Regan, B., & Grätzel, M. (1991). A Low-cost, high-efficiency solar cell based on dye-sensitized colloidal TiO_2 films. *Nature, 353,* 737-740.

[15] Buraidah, M.H., Teo, L.P., Yusuf, S.N.F., Noor, M.M., Kufian, M.Z., Careem, M.A., *et al.* (2011). TiO_2/ Chitosan-$NH_4I(+I_2)$-BMII-based dye-sensitized solar cells with anthocyanin dyes extracted from black rice and red cabbage. *International Journal of Photoenergy,* Vol. 2011, Article ID 273683, 11 pages.

[16] Noor, M.M., Buraidah, M.H., Yusuf, S.N.F., Careem, M.A., Majid, S.R., & Arof, A.K. (2011). Performance of dye-sensitized solar cells with (PVDF-HFP)-KI-EC-PC electrolyte and different dye materials. *International Journal of Photoenergy,* Vol. 2011, Article ID 960487, 5 pages.

[17] Kim, S., Lee, J.K., Kang, S.O., Ko, J., Yum, J.-H., Fantacci, S., *et al.* (2008). Molecular engineering of organic sensitizers for solar cell applications. *Journal of the American Chemical Society, 128,* 16701-16707.

[18] Vogel, R., Pohl, K., & Weller, H. (1990). Sensitization of highly porous, polycrystalline TiO_2 electrodes by quantum sized CdS. *Chemical Physics Letters, 174,* 241-246.

[19] Vogel, R., Hoyer, P., & Weller, H. (1994). Quantum-sized PbS, CdS, Ag_2S, Sb_2S_3 and Bi_2S_3 particles as sensitizers for various nanoporous wide-bandgap semiconductors. *Journal of Physical Chemistry, 98,* 3183-3188.

[20] Kamat, P.V. (2008). Quantum dot solar cells. Semiconductor nanocrystals as light harvesters. *Journal of Physical Chemistry C, 112,* 18737-18753.

[21] Rühle, S., Shalom, M., & Zaban, A. (2010). Quantum-dot-sensitized solar cells. *ChemPhysChem, 11,* 2290-2304.

[22] Yu, W., Qu, L.H., Guo, W.Z., & Peng, X.G. (2003). Experimental determination of the extinction coefficient of CdTe, CdSe, and CdS nanocrystals. *Chemistry of Materials, 15,* 2854–2860.

[23] Gonzalez-Pedro, V., Xu, X., Mora-Sero, I., & Bisquert, J. (2010). Modeling high-efficiency quantum dot sensitized solar cells. *ACS Nano, 4,* 5783-5790.

[24] Im, J.-H., Lee, C.-R., Lee, J.-W., Park, S.-W., & Park, N.-G. (2011). 6.5% efficient perovskite quantum-dot-sensitized solar cell. *Nanoscale, 3,* 4088-4093.

[25] Ip, A.H., Thon, S.M., Hoogland, S., Voznyy, O., Zhitomirsky, D., Debnath, R., *et al.* (2012). Hybrid passivated colloidal quantum dot solids. *Nature Nanotechnology, 7,* 577-582.

[26] Chang, J.-Y., Su, L.-F., Li, C.-H., Chang, C.-C., & Lo, J.-M. (2012). Efficient "green" quantum dot-sensitized solar cells based on Cu_2S-$CuInS_2$-ZnSe architecture. *Chemical Communications, 48,* 4848-4850.

[27] Peter, L.M. (2011). The Gratzel cell: Where next? *Journal of Physical Chemistry Letters, 2*, 1861-1867.

[28] Grätzel, M. (2004). Conversion of sunlight to electric power by nanocrystalline dye-sensitized solar cells. *Journal of Photochemistry and Photobiology A: Chemistry*, *164*, 3-14.

[29] Tennakone, K., Kumara, G.R.R.A., Kottegoda, I.R.M., & Perera, V.P.S. (1999). An efficient dye-sensitized photoelectrochemical solar cell made from oxides of tin and zinc. *Chemical Communications*, 15-16.

[30] Sayama, K., Sugihara, H., & Arakawa, H. (1998). Photoelectrochemical properties of a porous Nb_2O_5 electrode sensitized by a ruthenium dye. *Chemistry of Materials, 10,* 3825-3832.

[31] Nozik, A.J. (2002). Quantum dot solar cells. *Physica, E14,* 115-120.

[32] Zaban, A., Micic, O.I., Gregg, B.A., & Nozik, A.J. (1998). Photosensitization of nanoporous TiO_2 electrodes with InP quantum dots. *Langmuir, 14,* 3153-3156.

[33] Liu, D., & Kamat, P.V. (1993). Photoelectrochemical behaviour of thin CdSe and coupled TiO_2/CdSe semiconductor films. *Journal of Physical Chemistry, 97,* 10769-10773.

[34] Hoyer, P., & Konenkamp, R. (1995). Photoconduction in Porous TiO_2 Sensitized by PbS Quantum Dots. *Applied Physics Letters, 66,* 349-351.

[35] Yang, Z., Chen, C.-Y., Roy, P., & Chang, H.-T. (2011). Quantum dot-sensitized solar cells incorporating nanomaterials. *Chemical Communications, 47,* 9561-9571.

[36] Shalom, M., Tachan, Z., Bouhadana, Y., Barad, H.-N., & Zaban, A. (2011). Illumination intensity-dependent electronic properties in quantum dot sensitized solar cells. *Journal of Physical Chemistry Letters, 2,* 1998-2003.

[37] Robel, I., Subramanian, V., Kuno, M., & Kamat, P.V. (2006). Quantum dot solar cells. Harvesting light energy with CdSe nanocrystals molecularly linked to mesoscopic TiO_2 films. *Journal of the American Chemical Sociecty, 128,* 2385-2393.

[38] Robel, I., Kuno, M., & Kamat, P.V. (2007). Size-dependent electron injection from excited CdSe quantum dots into TiO_2 nanoparticles. *Journal of the American Chemical Society, 129,* 4136-4137.

[39] Kongkanand, A., Tvrdy, K., Takechi, K., Kuno, M., & Kamat, P.V. (2008). Quantum dot solar cells. Tuning photoresponse through size and shape control of CdSe-TiO_2 architecture. *Journal of the American Chemical Society, 130,* 4007-4015.

[40] Chakrapani, V., Tvrdy, K., & Kamat, P.V. (2010). Modulation of electron injection in CdSe-TiO_2 system through medium alkanility. *Journal of the American Chemical Society, 132*, 1228-1229.

[41] Mora-Sero, I., Bisquert, J., Dittrich, Th., Belaidi, A., Susha, A.S., & Rogach, A.L. (2007). Photosensitization of TiO_2 layers with CdSe quantum dots: correlation between light absorption and photoinjection. *Journal of Physical Chemistry C, 111,* 14889-14892.

[42] Shen, Y.-J., & Lee, Y.-L. (2008). Assembly of CdS quantum dots onto mesoscopic TiO_2 films for quantum dot-sensitized solar cell application. *Nanotechnology, 19*, 045602.

[43] Wang, X., Koleilat, G.I., Tang, J., Liu, H., Kramer, I.J., Debnath, R., *et al.* (2011). Tandem colloidal quantum dot solar cells employing a graded recombination layer. *Nature Photonics, 5*, 480-484.

[44] Peng, Z.A., & Peng, X. (2001). Formation of high-quality CdTe, CdSe, and CdS nanocrystals using CdO as precursor. *Journal of the American Chemical Society, 123*, 183-184.

[45] Grätzel, M. (2001). Photoelectrochemical cells. *Nature, 414,* 338-344.

[46] Gorer, S., & Hodes, G. (1994). Quantum size effects in the study of chemical solution deposition mechanism of semiconductor films. *Journal of Physical Chemistry, 98,* 5338-5346.

[47] Thambidurai, M., Muthukumarasamy, N., Agilan, S., Murugan, N., Vasantha, S., Balasundaraprabhu, R., *et al.* (2010). Strong quantum confinement effect in nanocrystalline CdS. *Journal of Materials Science*, *25,* 3254-3258.

[48] Nozik, A.J. (2005). Exciton multiplication and relaxation dynamics in quantum dots: Applications to ultrahigh-efficiency solar photon conversion. *Inorganic Chemistry, 44*, 6893-6899.

[49] Schaller, R.D., & Klimov, V.I. (2004). High efficiency carrier multiplication in PbSe nanocrystals: Implications for solar energy conversion. *Physical Review Letters, 92*, 186601.

[50] Ellingson, R.J., Beard, M.C., Johnson, J.C., Yu, P., Micic, O.I., Nozik, A.J., *et al.* (2005). Highly efficient multiple exciton generation in colloidal PbSe and PbS quantum dots. *Nano Letters, 5,* 865-871.

[51] Nozik, A.J., Beard, M.C., Luther, J.M., Law, M., Ellingson, R.J., & Johnson, J.C. (2010). Semiconductor quantum dots and quantum dot arrays and applications of multiple exciton generation to third-generation photovoltaic solar cells. *Chemical Reviews, 110,* 6873-6890.

[52] Beard, M.C. (2011). Multiple exciton generation in semiconductor quantum dots. *Journal of Physical Chemistry Letters, 2,* 1282-1288.

[53] Htoon, H., Malko, A.V., Bussian, D., Vela, J., Chen, Y., Hollingsworth, J.A., *et al.* (2010). Highly emissive multiexcitons in steady-state photoluminescence of individual “giant” CdSe/CdS core/shell nanocrystals. *Nano Letters, 10,* 2401-2407.

[54] Semonin, O.E., Luther, J.M., Choi, S., Chen, H.-Y., Gao, J., Nozik, A.J., *et al.* (2011). Peak external photocurrent quantum efficiency exceeding 100% via MEG in a quantum dot solar cell. *Science, 334,* 1530-1533.

[55] Nair, G., & Bawendi, M.G. (2007). Carrier multiplication yields of CdSe and CdTe nanocrystals by transient photoluminescence spectroscopy. *Physical Review B: Condensed Matter and Materials Physics, 76,* 081304.

[56] Scheller, R.D., Sykora, M., Jeong, S., & Klimov, V.I. (2006). High-efficiency carrier multiplication and ultrafast charge separation in semiconductor nanocrystals studied via time-resolved photoluminescence. *Journal of Physical Chemistry B, 110,* 25332-25338.

[57] Califano, M. (2011). Photoinduced surface trapping and the observed carrier multiplication yields in static CdSe nanocrystal samples. *ACS Nano, 5,* 3614-3621.

[58] Hanna, M.C., & Nozik, A.J. (2006). Solar conversion efficiency of photovoltaic and photoelectrolysis cells with carrier multiplication absorbers. *Journal of Applied Physics Letters, 100,* 074510.

[59] Emin, S., Singh, S.P., Han, L., Satoh, N., & Islam, A. (2011). Colloidal quantum dot solar cells. *Solar Energy, 85,* 1264-1282.

[60] Chen, H., Li, W., Liu, H., & Zhu, L. (2010). A suitable deposition method of CdS for high performance CdS-sensitized ZnO electrodes: Sequential chemical bath deposition *Solar Energy, 84,* 1201-1207.

[61] Zhu, G., Pan, L., Xu, T., & Sun, Z. (2011). Microwave assisted chemical bath deposition of CdS on TiO_2 film for quantum dot-sensitized solar cells. *Journal of Electroanalytical Chemistry, 659,* 205-208.

[62] Zhu, G., Pan, L., Xu, T., & Sun, Z. (2011). CdS/CdSe-cosensitized TiO2 photoanode for quantum-dot-sensitized solar cells by a microwave-assisted chemical bath deposition method. *ACS Applied Materials and Interfaces, 3,* 3146-3151.

[63] Pathan, H.M., & Lokhande, C.D. (2004). Deposition of metal chalcogenide thin films by successive ionic layer adsorption and reaction (SILAR) method. *Bulletin of Materials Science*, 27, 85-111.

[64] Senthamilselvi, V., Saravanakumar, K., Begum, N.J., Anandhi, R., Ravichandran, A.T., Sakthivel, B., *et al.* (2012). Photovoltaic properties of nanocrystalline CdS films deposited by SILAR and CBD techniques – a comparative study. *Journal of Materials Science: Materials in Electronics, 23,* 302-308.

[65] Toyoda, T., Sato, J., & Shen, Q. (2003). Effect of sensitization by quantum-sized CdS on photoacoustic and photoelectrochemical current spectra of porous TiO_2 electrodes. *Review of Scientific Instruments, 74,* 297-299.

[66] Lee, H.J., Wang, M., Chen, P., Gamelin, D.R., Zakeeruddin, S.M., Grätzel, M., *et al.* (2009). Efficient CdSe quantum dot-sensitized solar cells prepared by an improved successive ionic layer adsorption and reaction process. *Nano Letters, 9,* 4221-4227.

[67] Barcelo, I., Lana-Villarreal, T., & Gómez, R. (2011). Efficient sensitization of ZnO nanoporous films with CdSe QDs grown by successive ionic layer adsorption and reaction (SILAR). *Journal of Photochemistry and Photobiology A: Chemistry, 220,* 47-53.

[68] Qian, S., Wang, C., Lu, W., Zhu, Y., Yao, W., & Lu, X. (2011). An enhanced CdS/TiO_2 photocatalyst with high stability and activity: Effect of mesoporous substrate and bifunctional linking molecule. *Journal of Materials Chemistry, 21,* 4945-4952.

[69] Murray, C.B., Norris, D.J., & Bawendi, M.G. (1993). Synthesis and characterization of nearly monodisperse CdE (E = S, Se, Te) semiconductor nanocrystallites. *Journal of the American Chemical Society, 115,* 8706-8715.

[70] Gimenez, S., Mora-Sero, I., Macor, L., Guijarro, N., Lana-Villarreal, T., Gómez, R., *et al.* (2009). Improving the performance of colloidal quantum-dot-sensitized solar cells. *Nanotechnology, 20,* 295204.

[71] Guijarro, N., Lana-Villarreal, T., Mora-Sero, I., Bisquert, J., & Gómez, R. (2009). CdSe quantum dot-sensitized TiO_2 electrodes: Effect of quantum dot coverage and mode of attachment. *Journal of Physical Chemistry C, 113,* 4208-4214.

[72] Wijayantha, K.G.U., Peter, L.M., & Otley, L.C. (2004). Fabrication of CdS quantum dot sensitized solar cells via a pressing route. *Solar Energy Materials and Solar Cells, 83,* 363-369.

[73] Salant, A., Shalom, M., Hod, I., Faust, A., Zaban, A., & Banin, U. (2010). Quantum dot sensitized solar cells with improved efficiency prepared using electrophoretic deposition. *ACS Nano, 4,* 5962-5968.

[74] Poulose, A.C., Veeranarayanan, S., Varghese, S.H., Yoshida, Y., Maekawa, T., & Kumar, D.S. (2012). Functionalized electrophoretic deposition of CdSe quantum dots onto TiO_2 electrode for photovoltaic application. *Chemical Physics Letters, 539-540,* 197-203.

[75] Lee, Y.H., Im, S.Y., Lee, J.-H., & Seok, S.I. (2011). Porous CdS-sensitized electrochemical solar cells. *Electrochimica Acta, 56,* 2087-2091.

[76] Zhu, G., Lv, T., Pan, L., Sun, Z., & Sun, C. (2011). All spray pyrolysis deposited CdS sensitized ZnO films for quantum dot-sensitized solar cells. *Journal of Alloys and Compounds, 509,* 362-365.

[77] Kashyout, A.B., Soliman, H.M.A., Fathy, M., Gomaa, E.A., & Zidan, A.A. (2012). CdSe quantum dots for solar cell devices. *International Journal of Photoenergy,* Vol. 2012, Article ID 952610, 7 pages.

[78] Zhu, L., An, W.-J., Springer, J.W., Modesto-Lopez, L.B., Gullapalli, S., Holten, D., *et al.* (2012). Linker-free quantum dot sensitized TiO_2 photoelectrochemical cells. *International Journal of Hydrogen Energy, 37,* 6422-6430.

[79] Joo, J., Kim, D., Yun, D.-J., Jun, H., Rhee, S.-W., Lee, J.S., *et al.* (2010). The fabrication of highly uniform ZnO/CdS core/shell structures using a spin-coating-based successive ion layer adsorption and reaction method. *Nanotechnology, 21,* 325604.

[80] Mora-Sero, I., & Bisquert, J. (2010). Breakthroughs in the development of semiconductor-sensitized solar cells. *Journal of Physical Chemistry Letters, 1,* 3046-3052.